

Fluorescent Imaging for Cysteine Detection In Vivo with High Selectivity

Zhuwen Duan^{+, [a]}, Youming Zhu^{+, [a]}, Yuyun Yang,^[a] Zixu He,^[a] Ju Liu,^{*, [a, b]} Ping Li,^{*, [a]} Hui Wang,^{*, [a]} and Bo Tang^[a]

As an essential amino acid, cysteine is involved in various biosynthetic and metabolic processes, such as protein synthesis, hormone synthesis, and redox homeostatic maintenance. Inordinate cysteine levels are often associated with serious diseases. Thus, designing and synthesizing a novel fluorescent probe for determining the concentration of cellular cysteine, which could indirectly monitor the prevalence of these diseases, is essential. We developed a fluorescence probe P-Cy with good

sensitivity for cysteine detection in vivo. P-Cy only exhibited good response toward cysteine but did not show response toward other biothiols, such as homocysteine (Hcy) and glutathione (GSH). In this study, we used P-Cy by successfully imaging cellular endogenous and exogenous cysteine levels. Furthermore, P-Cy was also performed in mice to detect cysteine level, indicating that P-Cy is a powerful tool for cysteine detection in situ.

1. Introduction

Cysteine is an essential biothiol in organisms that plays many crucial roles in metabolism.^[1-4] Cysteine is not only an essential amino acid in protein synthesis but also reacts to form a disulfide bond to maintain protein spatial structure.^[5-7] Furthermore, cysteine plays a significant role in maintaining redox homeostasis.^[8,9] Inordinate cysteine levels are often associated with serious diseases, including abnormal hematopoiesis, Alzheimer's disease, neurotoxicity, and liver damage.^[10-13] Given that cysteine, GSH, and Hcy contain sulfhydryl, specifically differentiating cysteine from GSH and Hcy is difficult.^[14-20] Hence, developing a fluorescent probe with high selectivity for cysteine detection in vivo is necessary.

Fluorescence imaging technology had been widely used in the past decades for in vivo imaging of reactive oxygen species (ROS)^[21-23] and reactive nitrogen species (RNS)^[24,25] because of its numerous advantages, such as reduced phototoxicity, real-time and in situ imaging, high selectivity, and good sensitivity.^[26-33]

Therefore, a new and easily synthesized fluorescence probe should be developed to monitor the cysteine level in situ and in real time.

In the present study, we synthesized the new fluorescence probe called P-Cy to image the cysteine level. P-Cy was designed following a photo-induced electron transfer (PET) principle.^[26,34,35] Merocyanine (Cy-Ph) was used as chromophore due to its extraordinary optical properties^[36] and acryloyl as recognition group.^[26,37,38] When cysteine was absent, the PET-induced quenching effect caused inconspicuous fluorescence intensity (FI) of P-Cy. After reaction with cysteine, P-Cy emitted bright fluorescence due to PET blocking (Figure 1). P-Cy could be easily synthesized in the lab with high yield of 63.16% under mild conditions. The ¹H NMR, ¹³C NMR and HRMS data were shown in supporting information. The fluorescence probe P-Cy was successfully applied to cysteine imaging in vitro with high selectivity and good sensitivity, both in cells and in vivo.

2. Results and Discussion

The absorption and emission spectra of TP-Cy in physiological condition was measured to understand its OP and TP fluorescence properties. The probe showed the maximum absorption peak at 520 nm (Figure 2a), and the emission peak was at 557 nm when it was excited at 520 nm in PBS buffer (pH 7.4). After reaction with cysteine in PBS buffer at 37 °C (pH = 7.4, 0.5% DMSO, v/v), the emission fluorescence intensity (FI) of P-Cy (5 μM) was significantly enhanced at 557 nm accompanied with increased fluorescence quantum yield (from 0.16 to 0.52). These data supported the design principle of the probe, causing PET to become blocked after reaction with cysteine followed by fluorescent recovery.

Subsequently, the correlation between FI and cysteine concentration was investigated. As shown in Figure 2b, along with the incremental concentration of cysteine (0 to 150 μM) reacting with 5 μM P-Cy in PBS, the FI of the reaction product

[a] Z. Duan,⁺ Y. Zhu,⁺ Y. Yang, Z. He, Prof. J. Liu, Prof. P. Li, Dr. H. Wang, Prof. B. Tang
College of Chemistry, Chemical Engineering and Materials Science, Institute of Biomedical Sciences, Collaborative Innovation Center of Functionalized Probes for Chemical Imaging in Universities of Shandong, Key Laboratory of Molecular and Nano Probes, Ministry of Education, Shandong normal University, Jinan 250014, PR China
E-mail: eastlodge1999@163.com
lip@sdu.edu.cn
hui_wang@sdu.edu.cn

[b] Prof. J. Liu
Medical Research Center, Shandong Provincial Qianfoshan Hospital, Shandong University, Jinan 250014, PR China

[⁺] These authors contribute equally to this work.

Supporting information for this article is available on the WWW under <https://doi.org/10.1002/open.201900045>

© 2019 The Authors. Published by Wiley-VCH Verlag GmbH & Co. KGaA.
This is an open access article under the terms of the Creative Commons Attribution Non-Commercial License, which permits use, distribution and reproduction in any medium, provided the original work is properly cited and is not used for commercial purposes.

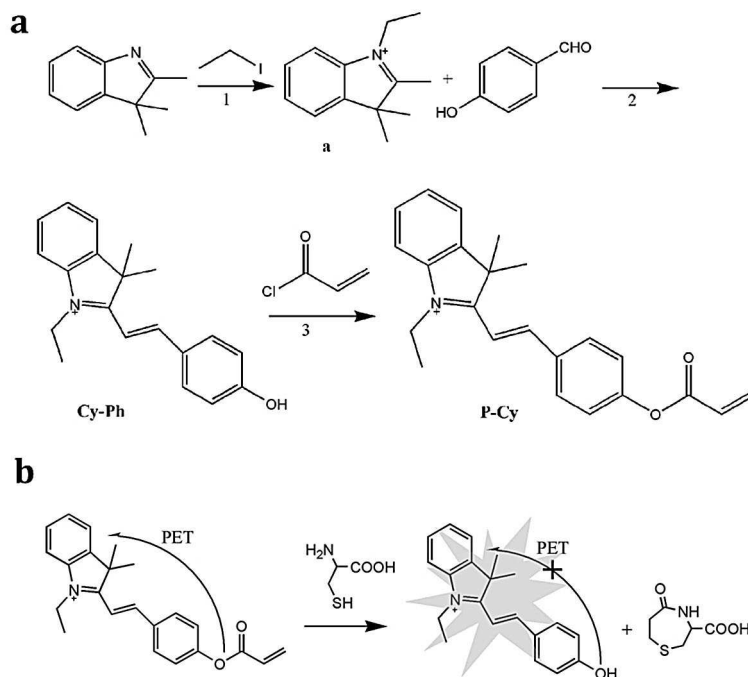


Figure 1. Schematic design and recognition mechanism of P-Cy.

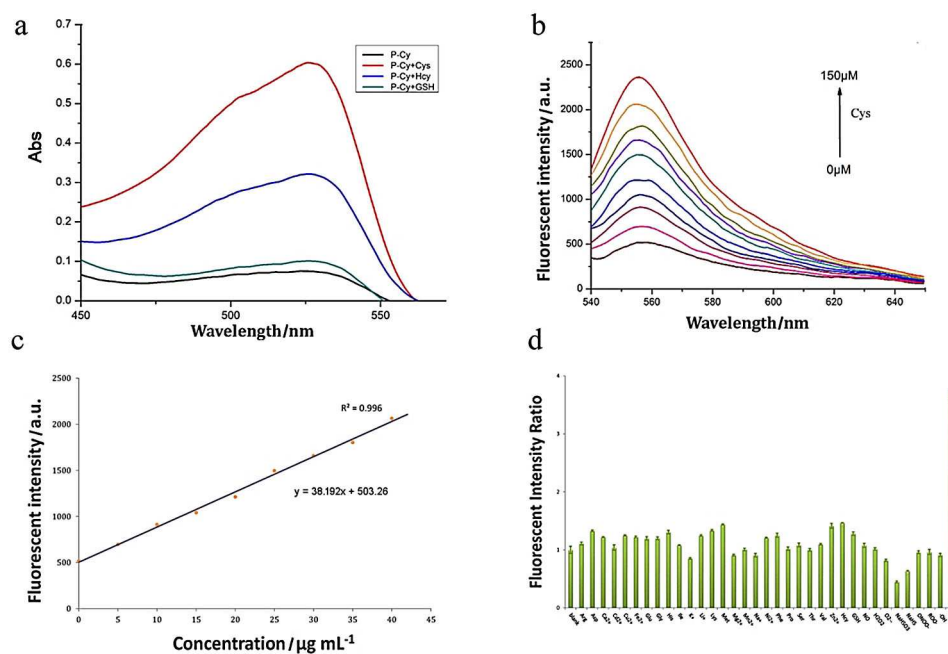


Figure 2. Photophysical properties and selectivity of P-Cy. (a) Absorption spectra of P-Cy when cysteine, GSH and Hcy present or absent. (b) Fluorescent spectra of P-Cy with increasing concentration of cysteine. (c) Linear relationship between FI of P-Cy and cysteine. (d) Fluorescence responses of P-Cy to different competing species: ROS, RNS, RSS, Ca^{2+} , Cd^{2+} , Cu^{2+} , Fe^{2+} , K^{+} , Li^{2+} , Mg^{2+} , Mn^{2+} , Na^{+} , Ni^{2+} , Arg, Asp, Glu, Gly, His, Ile, Lys, Met, Phe, Pro, Ser, Thr, Val, Hcy, GSH and cysteine. Error bars represent standard deviation ($n = 3$).

gradually increased. We made a scatter plot by utilizing the cysteine concentration and FI data. We found that they exhibited a good linear relationship with $R^2 = 0.996$ (Figure 2c). The limit of detection (LOD) of P-Cy was calculated as $0.82 \mu\text{M}$. These results showed that P-Cy had an excellent response to cysteine in physiological conditions, and its FI could reflect the

cysteine concentration. Then, the P-Cy response toward cysteine under fluctuant pH in physiological range (5.0-8.0) was investigated (Figure S2), suggesting that the P-Cy probe could be used in vivo to sense the cysteine fluctuation in neutral pH.

We examined whether other relative biotic components interfered with P-Cy and cysteine reaction. We tested the

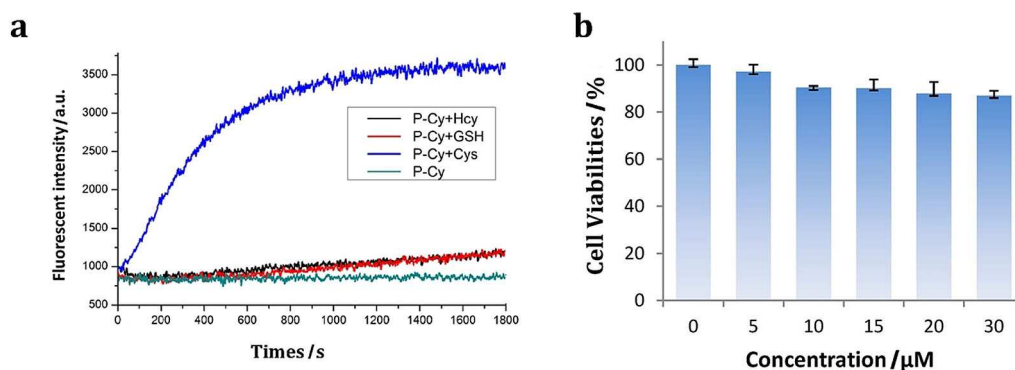


Figure 3. The photostability and cytotoxicity of P-Cy. (a) The FI of free P-Cy and P-Cy with cysteine, GSH and Hcy in 30 min. (b) The cytotoxicity of P-Cy were tested by MTT assay. Error bars represent standard deviation ($n = 3$).

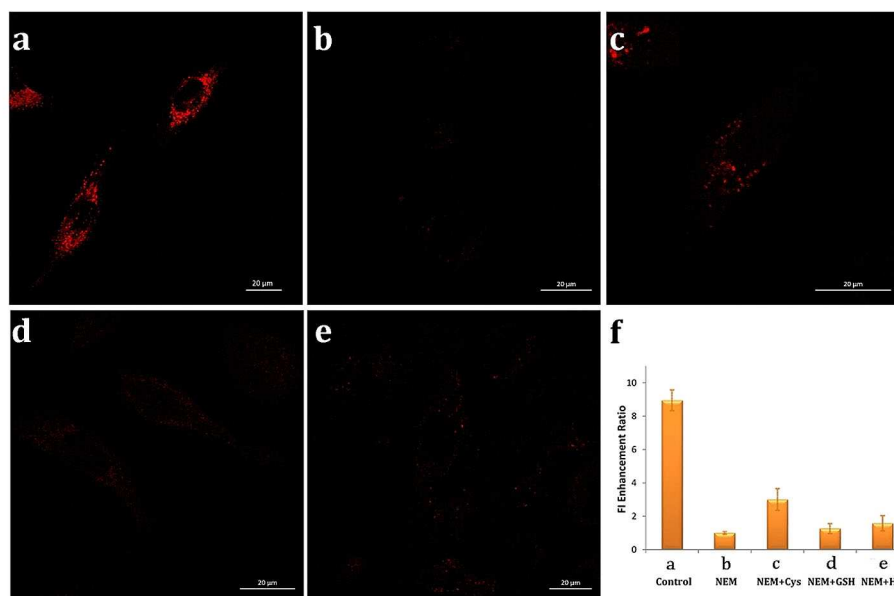


Figure 4. Fluorescence images of P-Cy in A549 cells. (a) Control group cells. (b) NEM group cells. (c) Cysteine group cells. (d) GSH group cells. (e) Hcy group cells. (f) FI of P-Cy in different groups of cell. All cells were incubated with 5 μM P-Cy for 10 min before imaging. $\lambda_{\text{ex}} = 514 \text{ nm}$; $\lambda_{\text{em}} = 540\text{--}650 \text{ nm}$. Scale bar = 10 μm. Error bars represent standard deviation ($n = 5$).

response of P-Cy toward various ROS (H_2O_2 , $\cdot\text{OH}$ and $\text{O}_2^{\cdot-}$), RNS (NO, ONOO $^-$ and ROO \cdot), RSS (NaHSO $_3$ and NaHS), amino acids, metal ions, GSH and Hcy. As shown in Figure 2d and Figure S3, scarcely any influence on P-Cy fluorescence was observed after the addition of these interfering species, indicating that P-Cy possessed extremely high selectivity toward cysteine. Besides, the photostability and cytotoxicity of P-Cy were investigated (Figure 3). The results showed that the FI of P-Cy with cysteine reached the platform in 10 min and exhibited stable FI for at least 20 min. In addition, no obvious cytotoxicity was observed by the tetrazolium based colorimetric (MTT) assay when 30 μM P-Cy was used.

The application of P-Cy as fluorescent probe for cysteine imaging in cells was evaluated. The probe was used in human lung adenocarcinoma cells (A549) for the fluorescent imaging of endogenous and exogenous cysteine. The cells were divided to five groups, and a thiol-blocking reagent N-ethylmaleimide^[39]

(NEM, 1 mM) was incubated with each group of cells, except the control group, before P-Cy (5 μM) was loaded. As shown in Figure 4a, prominent fluorescence was shown in control group cells, which was only incubated with P-Cy, indicating that P-Cy could successfully sense the endogenous cysteine level in the cell. Then NEM was pretreated with cells for 30 min to clear the endogenous thiols, and nearly no fluorescence was observed (Figure 4b), suggesting that extremely low concentration of cysteine was left after NEM incubation (8.9-fold decrease than control group). Subsequently, cysteine (1 mM), GSH (10 mM), and Hcy (10 mM) were incubated with NEM-pretreated cells respectively. Figure 4d and 4e shows that although high concentrations of GSH (1.1-fold enhancement than NEM-cells) and Hcy (1.3-fold) were added into cell incubation buffer, the FI of P-Cy was still faint. However, when NEM-pretreated A549 cells were incubated with 1 mM cysteine (Figure 4c), significant fluorescence was observed (3.4-fold), proving that P-Cy could

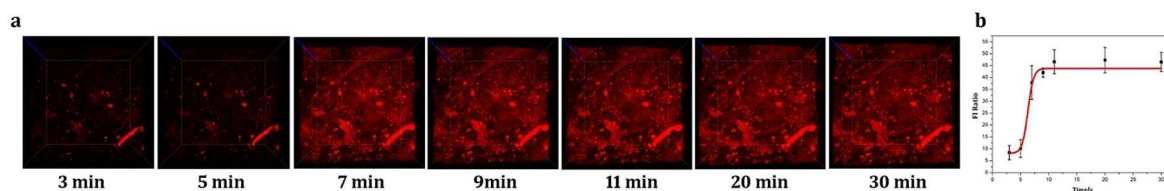


Figure 5. Fluorescent imaging of cysteine in mice with increasing time. (a) Fluorescent imaging of P–Cy (20 μ M) response to cysteine with different time. (b) FI of P–Cy from images ($\lambda_{\text{ex}} = 514$ nm; $\lambda_{\text{em}} = 540\text{--}650$ nm). Scale bar = 20 μ m. Error bars represent standard deviation (n = 5).

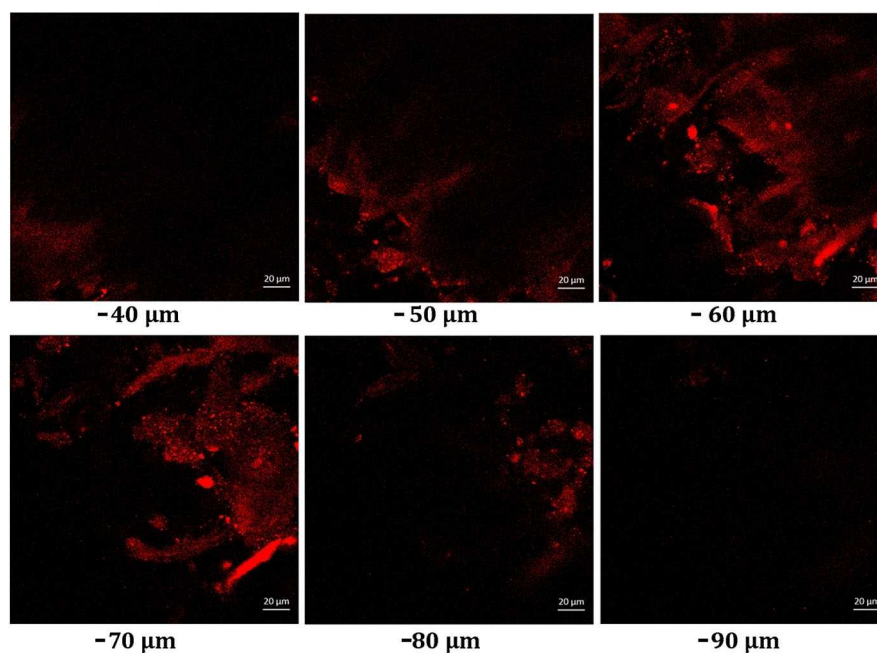


Figure 6. Fluorescent imaging of cysteine in mice in vivo. $\lambda_{\text{ex}} = 514$ nm; $\lambda_{\text{em}} = 540\text{--}650$ nm. Scale bar = 20 μ m.

detect exogenous cysteine in cells. These imaging data demonstrated that P–Cy was capable of imaging endogenous and exogenous cysteine level in cells with high selectivity in real-time.

Because of the outstanding performance of P–Cy on cysteine imaging in cells, we employed it to image cysteine in vivo under 514 nm excitation. The 16–18 g female BALB/c mice were used and injected with P–Cy (25 μ M, 100 μ L) into the abdomens of mice. All mice were purchased from The Animal Living Center of Shandong University. The animal experiments were approved in compliance with the relevant laws and guidelines issued by the Ethical Committee of Shandong University and were in agreement with the guidelines of the Institutional Animal Care and Use Committee. As shown in Figure 5, the red fluorescence gradually increased over time with 514 nm excitation, reaching the platform with the strongest fluorescence intensity at 9 min. Then we scanned the fluorescence imaging depth, as shown in Figure 6, the fluorescence imaging depth reached to maximum 80 μ m. This result demonstrated that P–Cy could be applied for cysteine detection in vivo.

In summary, we described the new easily synthesized fluorescence probe P–Cy for cysteine detection in vitro and in vivo. P–Cy could be used for the fluorescence imaging of cysteine in cells and in vivo with high selectivity, good sensitivity, and low cytotoxicity. With these outstanding advantages, the probe possesses enough superiority to be commercially produced in the future. We believe the P–Cy can be a practical tool as a cysteine indicator in biological and clinical medical research.

Acknowledgements

This work was supported by National Natural Science Foundation of China (21405097) and the Primary Research Plan in Shandong Province (Grant NO. 2016GSF201205).

Conflict of interest

There are no conflicts to declare.

Keywords: cysteine · in vivo detection · fluorescence imaging · biothiols · probes

- [1] S. P. Baba, A. Bhatnagar, *Curr. Opin. Toxicol.* **2018**, *7*, 133–139.
- [2] M. H. Akabas, *Adv. Exp. Med. Biol.* **2015**, *869*, 25–54.
- [3] F. C. Bi, Q. F. Zhang, Z. Liu, C. Fang, J. Li, J. B. Su, J. T. Greenberg, H. B. Wang, N. Yao, *PLoS One* **2011**, *6*, e18079.
- [4] D. G. Isom, E. Vardy, T. G. Oas, H. W. Hellinga, *Proc. Natl. Acad. Sci. USA* **2010**, *107*, 4908–4913.
- [5] R. J. Mailloux, X. Jin, W. G. Willmore, *Redox Biol.* **2014**, *2*, 123–139.
- [6] C. L. Oeste, D. Perez-Sala, *Mass Spectrom. Rev.* **2014**, *33*, 110–125.
- [7] J. Hu, Z. Zhang, W. J. Shen, A. Nomoto, S. Azhar, *Biochemistry* **2011**, *50*, 10860–10875.
- [8] D. Spadaro, B. W. Yun, S. H. Spoel, C. Chu, Y. Q. Wang, G. J. Loake, *Physiol. Plant.* **2010**, *138*, 360–371.
- [9] N. M. Giles, A. B. Watts, G. I. Giles, F. H. Fry, J. A. Littlechild, C. Jacob, *Chem. Biol.* **2003**, *10*, 677–693.
- [10] G. Schunzel, G. L. Riutrikh, W. Schmidt, *Med. Radiol. (Mosk)* **1976**, *21*, 60–61.
- [11] S. Hasanbasic, A. Jahic, E. Karahmet, A. Sejranic, B. Prnjavorac, *Mater. Sociomed.* **2016**, *28*, 235–238.
- [12] Y. I. Mahmoud, S. S. Sayed, *Biotech. Histochem.* **2016**, *91*, 327–332.
- [13] R. Janaky, V. Varga, A. Hermann, P. Saransaari, S. S. Oja, *Neurochem. Res.* **2000**, *25*, 1397–1405.
- [14] H. S. Jung, J. H. Han, T. Pradhan, S. Kim, S. W. Lee, J. L. Sessler, T. W. Kim, C. Kang, J. S. Kim, *Biomaterials* **2012**, *33*, 945–953.
- [15] H. Y. Shiu, H. C. Chong, Y. C. Leung, M. K. Wong, C. M. Che, *Chemistry* **2010**, *16*, 3308–3313.
- [16] M. Wei, P. Yin, Y. Shen, L. Zhang, J. Deng, S. Xue, H. Li, B. Guo, Y. Zhang, S. Yao, *Chem. Commun. (Camb.)* **2013**, *49*, 4640–4642.
- [17] D. Chen, Z. Long, Y. Dang, L. Chen, *Analyst* **2018**, *143*, 5779–5784.
- [18] L. Fan, W. Zhang, X. Wang, W. Dong, Y. Tong, C. Dong, S. Shuang, *Analyst* **2019**, *144*, 439–447.
- [19] X. Yang, W. Liu, J. Tang, P. Li, H. Weng, Y. Ye, M. Xian, B. Tang, Y. Zhao, *Chem. Commun. (Camb.)* **2018**, *54*, 11387–11390.
- [20] X. Chen, Y. Zhou, X. Peng, J. Yoon, *Chem. Soc. Rev.* **2010**, *39*, 2120–2135.
- [21] X. L. Hao, Z. J. Guo, C. Zhang, A. M. Ren, *Phys. Chem. Chem. Phys.* **2018**, *21*, 281–291.
- [22] Y. Lu, X. Shi, W. Fan, C. A. Black, Z. Lu, C. Fan, *Spectrochim. Acta Part A Mol. Biomol. Spectrosc.* **2018**, *190*, 353–359.
- [23] M. D. Li, N. K. Wong, J. Xiao, R. Zhu, L. Wu, S. Y. Dai, F. Chen, G. Huang, L. Xu, X. Bai, M. R. Geraskina, A. H. Winter, X. Chen, Y. Liu, W. Fang, D. Yang, D. L. Phillips, *J. Am. Chem. Soc.* **2018**, *140*, 15957–15968.
- [24] S. J. Li, D. Y. Zhou, Y. Li, H. W. Liu, P. Wu, J. Ou-Yang, W. L. Jiang, C. Y. Li, *ACS Sens.* **2018**, *3*, 2311–2319.
- [25] X. Zhu, J. Q. Chen, C. Ma, X. Liu, X. P. Cao, H. Zhang, *Analyst* **2017**, *142*, 4623–4628.
- [26] C. Chen, L. Zhou, W. Liu, W. Liu, *Anal. Chem.* **2018**, *90*, 6138–6143.
- [27] X. L. Hao, Z. J. Guo, C. Zhang, A. M. Ren, *Phys. Chem. Chem. Phys.* **2018**, *21*, 281–291.
- [28] P. Kumari, S. K. Verma, S. M. Mobin, *Chem. Commun. (Camb.)* **2019**, *55*, 294–297.
- [29] C. Ma, M. Ma, Y. Zhang, X. Zhu, L. Zhou, R. Fang, X. Liu, H. Zhang, *Spectrochim. Acta Part A Mol. Biomol. Spectrosc.* **2018**, *212*, 48–54.
- [30] S. Yao, C. Ma, Y. Lu, X. Wei, X. Feng, P. Miao, G. Yang, J. Zhang, M. Yan, J. Yu, *Analyst* **2019**.
- [31] Y. M. W. L. Yuping Zhao, *Sens. Actuators B* **2018**, 157–163.
- [32] Y. Tang, Z. Wu, C. H. Zhang, X. L. Zhang, J. H. Jiang, *Chem. Commun. (Camb.)* **2016**, *52*, 3631–3634.
- [33] K. Gu, Y. Xu, H. Li, Z. Guo, S. Zhu, S. Zhu, P. Shi, T. D. James, H. Tian, W. H. Zhu, *J. Am. Chem. Soc.* **2016**, *138*, 5334–5340.
- [34] Y. Qi, Y. Huang, B. Li, F. Zeng, S. Wu, *Anal. Chem.* **2018**, *90*, 1014–1020.
- [35] K. Kunieda, H. Yamauchi, M. Kawaguchi, N. Ieda, H. Nakagawa, *Bioorg. Med. Chem. Lett.* **2018**, *28*, 969–973.
- [36] S. P. Wang, W. J. Deng, D. Sun, M. Yan, H. Zheng, J. G. Xu, *Org. Biomol. Chem.* **2009**, *7*, 4017–4020.
- [37] S. J. Li, Y. J. Fu, C. Y. Li, Y. F. Li, L. H. Yi, J. Ou-Yang, *Anal. Chim. Acta* **2017**, *994*, 73–81.
- [38] X. Jia, C. Niu, Y. He, Y. Sun, H. Liu, *J. Fluoresc.* **2018**, *28*, 1059–1064.
- [39] H. Zhang, N. Qin, Z. Fang, *Molecules* **2018**, *23*.

Manuscript received: January 29, 2019

Accepted: February 13, 2019